arXiv:1202.4167v1 [hep-ph] 19 Feb 2012

X(1835), X(2120) and X(2370) in a flux tube model

Chengrong Deng[1], Jialun Ping[2*], Youchang Yang[3], Fan Wang[4]
[1]*School of Mathematics and Physics, Chongqing Jiaotong University, Chongqing 400074, P.R. China*
[2]*Department of Physics, Nanjing Normal University, Nanjing 210097, P.R. China*
[3]*Department of Physics, Zunyi Normal College, Zunyi 563002, P.R. China and*
[4]*Department of Physics, Nanjing University, Nanjing 210093, P.R. China*

Nonstrange baryonium spectrum is systematically studied by using the Gaussian expansion method in a flux tube model with the six-body confinement potential. All the model parameters are fixed by baryon properties, so the baryonium calculation is parameter-free. We find that $X(1835)$ and $X(2370)$, which are observed in the radiative decay of J/ψ by BES collaboration, can be described as $N_8\bar{N}_8$ and $\Delta_8\bar{\Delta}_8$ bound states with quantum numbers $I^GJ^{PC}=0^+0^{-+}$, respectively, such bound states should be color confinement resonances with three-dimensional configurations similar to dumbbell, however, $X(2120)$ can not be accommodated in our model.

PACS numbers: 12.39.Jh, 13.75.Cs, 14.40.Rt

I. INTRODUCTION

In 2003, X(1860) was observed in the $p\bar{p}$ invariant mass spectrum in the radiative decay $J/\psi \to \gamma p\bar{p}$ by BES collaboration, the mass and the width are $M=1859^{+3+5}_{-10-20}$ MeV and Γ <30 MeV, respectively [1]. In 2005, $X(1835)$ was first observed in $J/\psi \to \gamma\pi^+\pi^-\eta'$ decays with a statistical significance of 7.7 σ by BESII [2], the parameters of $X(1835)$ are $M=1833.7\pm 6.5\pm 2.7$ MeV and $\Gamma=67.7\pm 20.3\pm 7.7$ MeV. Very recently, the $X(1835)$ was confirmed by BESIII in the radiative decay $J/\psi \to \gamma\pi^+\pi^-\eta'$ with mass and width $M=1836.5\pm 3.0^{+5.6}_{-2.1}$ MeV and $\Gamma=190\pm 9^{+38}_{-36}$ MeV, respectively [3]. The mass is consistent with the BESII result, while the width is significantly larger. Meanwhile, $X(2120)$ and $X(2370)$ were also observed in the same process, the masses and the widths are $M_{X(2120)}=2122.4\pm 6.7^{+4.7}_{-2.7}$ MeV, $M_{X(2370)}=2376.3\pm 8.7^{+3.2}_{-4.3}$ MeV, $\Gamma_{X(2120)}=83\pm 16^{+31}_{-11}$ MeV, and $\Gamma_{X(2370)}=83\pm 17^{+44}_{-6}$ MeV, respectively.

Many theoretical works were stimulated to interpret the natures and structures of the resonances. Datta and O'Donnell described $X(1860)$ as a zero baryon number, deuteron-like singlet $p\bar{p}$ $^0S_1$ state in a simple potential model with a $\lambda\cdot\lambda$ confining interaction [4]. Ding and Yan discussed $X(1860)$ as a baryonium and investigated mesonic decays of $X(1860)$ due to the nucleon-antinucleon annihilation [5]. Gao and Zhu understood $X(1860)$ as the $p\bar{p}$ bound state with quantum numbers $I^GJ^{PC}=0^+0^{-+}$, and demonstrated that which can not decay into final state $\pi^+\pi^-$, $2\pi^0$, $\bar{K}K$ and 3π [6]. Kochelev and Min explained $X(1835)$ as the lowest pseudoscalar glueball state due to the instanton mechanism of partial $U(1)_A$ symmetry restoration [7]. He *et al.* studied $X(1835)$ using the QCD sum rule and interpreted it as a pseudoscalar state with a large gluon content [8]. Li investigated $X(1835)$ as a 0^{-+} pseudoscalar glueball using an effective Lagrangian approach [9]. Ding *et al.* treated $X(1835)$ as a baryonium with a sizable gluon content [10]. Liu proposed that X(1835) contained a baryonium component from the large-N_c QCD point of view [11]. Dedonder *et al.* studied $X(1835)$ in the conventional $N\bar{N}$ potential model and suggested that it could be a broad and weakly bound state $N\bar{N}_s(1870)$ in the $^1S_0$ wave. Huang and Zhu treated X(1835) as the second radial excitation of $\eta'(958)$ and discussed the strong decay behavior by the effective Lagrangian approach [12]. Li and Ma studied several two-body strong decays of X(1835) associated with $\eta(1760)$ by the quark-pair-creation model, where $X(1835)$ is assigned as the $n^{2s+1}L_J=3^1S_0$ $q\bar{q}$ state. Entem and Fernández derived a $N\bar{N}$ interaction from a constituent quark model constrained by the NN sector to investigate the possible baryonium resonant state $X(1835)$ [13]. Yu *et al*'s study indicated that: (1) X(1835) could be the second radial excitation of $\eta'(958)$; (2) X(2120) and (2370) can be explained as the third and fourth radial excitations of $\eta(548)/\eta'(958)$ [14].

Quantum Chromodynamics (QCD) is widely accepted as the fundamental theory of strong interaction. Lattice QCD (LQCD) and nonperturbative QCD method have made impressive progresses on hadron properties, even on hadron-hadron interactions [15–17]. However, constituent quark model (CQM) is still an useful tool in obtaining physical insight for these complicated strong interaction systems. CQM can offer the most complete description of hadron properties and is probably the most successful phenomenological model of hadron structure [18]. Naive CQM based on two-body color confinement interaction proportional to the color charges can describe the properties of usual hadrons well because of their unique color structures. However, the structures of multiquark systems and hadron-hadron interactions are abundant [19–21], which have important information that is absent from ordinary hadrons. Thus there is no any theoretical reason to implement naive models directly to multi-quark systems. Furthermore the direct implementation may induce some serious problems, such

---

[*] Correponding author: J. Ping (jlping@njnu.edu.cn)

as anti-confinement and too strong color Van der Waals force [22]. Many theoretical works have been done to try to amend those serious drawbacks. The string flip model was proposed by M. Oka for multi-quark systems to avoid pathological Van der Waals force [23, 24]. Dmitrasinovic investigated the tetraquark system with the three-body $qq\bar{q}$ and $q\bar{q}\bar{q}$ interaction, whose existence has no direct effect on the ordinary hadron states [25].

LQCD allows us to investigate the confinement phenomenon in a nonperturbative framework. Its calculations for mesons, baryons, tetra-quarks and penta-quarks reveals flux-tube or string like structure [26, 27], the confinement of multi-quark states are multi-body interactions and can be simulated by a potential which proportional to the minimum of the total length of strings which connect the quarks to form a multiquark state. A naive flux-tube or string model basing on this picture has been constructed [19–21]. It takes into account of multi-body confinement with harmonic interaction approximation, i.e., where the length of string is replaced by the square of the length to simplify the numerical calculation. There are two arguments to expect this: One is that the spatial variations in separation of the quarks (lengths of the string) in different hadrons do not differ significantly, so the difference between the two functional forms is small and can be absorbed in the adjustable parameter, the stiffness. The second is that we are using a nonrelativistic description of the dynamics and, as was shown long ago [28], an interaction energy that varies linearly with separation between fermions in a relativistic, first order differential dynamics has a wide region in which a harmonic approximation is valid for the second order (Feynman-Gell-Mann) reduction of the equations of motion.

The flux tube model has been applied to the study of exotic mesons [20]. The results suggest that the multi-body confinement should be employed in the quark model study of multiquark states instead of the additive two-body confinement. The flux tube model with four-body confinement potential also described light scalar meson spectrum well in the framework of a tetraquark picture [29]. This paper extends the model to six-quark system, to investigate systematically the non-strange baryonium states with six-body confinement potential. The numerical results are obtained by Gaussian Expansion Method (GEM). The paper is organized as follows: the model Hamiltonian and wave-function for 3-quark system are presented in Sec. II. The six-body confinement potential and the wave-function of a six-quark system are introduced in Sec. III. Sect. IV presents the numerical results and discussions. We give a brief summary in the last section.

II. QUARK MODEL AND BARYON SPECTRUM

The model Hamiltonian for 3-quark system takes the form

$$
\begin{aligned}
H &= \sum_{i=1}^{3}\left(m_i+\frac{\mathbf{p}_i^2}{2m_i}\right)-T_{CM}+V^C+\sum_{i>j}^{3}V_{ij}^G, \quad (1)\\
V_{ij}^G &= \frac{1}{4}\alpha_s\lambda_i\cdot\lambda_j\left[\frac{1}{r_{ij}}-\frac{\pi}{2}\delta(\mathbf{r}_{ij})\right.\\
&\quad\times\left.\left(\frac{1}{m_i^2}+\frac{1}{m_j^2}+\frac{4}{3m_im_j}\sigma_i\cdot\sigma_j\right)\right], \quad (2)\\
V^C &= K\left((\mathbf{r}_1-\mathbf{y}_0)^2+(\mathbf{r}_2-\mathbf{y}_0)^2+(\mathbf{r}_3-\mathbf{y}_0)^2\right) \quad (3)
\end{aligned}
$$

where $\mathbf{r}_i$, m_i and $\mathbf{p}_i$ are the position, mass and momentum of the i-th quark and $\mathbf{y}_0$ is the position of the junction where three strings meet. T_C is the kinetic energy of the center-of-mass of the system. λ^c and σ are are the $SU(3)$ Gell-man and $SU(2)$ Pauli matrices, respectively; note that $\lambda\to-\lambda^*$ for anti-quark. An effective scale-dependent strong coupling constant [30] is used here

$$
\alpha_s(\mu)=\frac{\alpha_0}{\ln\left[\frac{\mu^2+\mu_0^2}{\Lambda_0^2}\right]} \quad (4)
$$

where μ is the reduced mass of two interactional quarks, and α_0, μ_0 and Λ_0 are determined in below discussion. The δ function, arising as a consequence of the non-relativistic reduction of the one-gluon exchange diagram between point-like particles, has to be regularized in order to perform numerical calculations. It reads [31]

$$
\delta(r_{ij})=\frac{1}{\beta^3\pi^{\frac{3}{2}}}e^{-r_{ij}^2/\beta^2}, \quad (5)
$$

where β is the model parameter which is determined by fitting the experiment data. For the confinement potential V^C, the position of the junction $\mathbf{y}_0$ can be fixed by minimizing the energy of the system and, we get

$$
\mathbf{y}_0=\frac{\mathbf{r}_1+\mathbf{r}_2+\mathbf{r}_3}{3} \quad (6)
$$

Therefore, the minimum of the confinement for 3-quark baryons V^C_{min} has the following forms

$$
V^C_{min}=K\sum_{i,j,k=1}^{3}{}'\frac{1}{3}\left[\left(\frac{\mathbf{r}_i-\mathbf{r}_j}{\sqrt{2}}\right)^2+\left(\frac{2\mathbf{r}_k-\mathbf{r}_i-\mathbf{r}_j}{\sqrt{6}}\right)^2\right] \quad (7)
$$

$\sum'$ denotes summing only over the cyclic permutations of $(1,2,3)$. In this work, the tensor forces and spin-orbit forces between quarks are omitted, since they are not effective in the baryon ground states.

For baryons, the color part wave function ψ_c is antisymmetrical because of the color singlet requirement. The spatial wave function $\psi^G_{L_TM_T}(\mathbf{R},\mathbf{r})$ is assumed to be symmetric because the states we are interested in are ground states. So the spin-flavor wave function $\psi_{IM_ISM_S}$, only the $SU(4) \supset SU_s(2) \times SU_f(2)$ symmetry is used here, are symmetric under the interchange of two identical particles. The total antisymmetrical wave function can be described as,

$$\Phi_{IM_IJM_J}(\mathbf{R},\mathbf{r}) = \psi_c \left[\psi^G_{L_TM_T}(\mathbf{R},\mathbf{r})\psi_{IM_ISM_S}\right]_{IM_IJM_J} \quad (8)$$

$[\cdots]_{IM_IJM_J}$ means coupling the spin S and total orbital angular momentum L_T with Clebsch-Gordan Coefficients. Because N, Δ and Ω are composed of three identical quarks, while other baryons, Λ, Σ, Σ^*, Ξ and Ξ^*, have two identical quarks, thus we introduce two different types of spatial wave functions. For N, Δ and Ω, we define Jacobian coordinates $\mathbf{r}_{ij}$ and $\mathbf{R}_k$ for the cyclic permutations of $(1,2,3)$.

$$\mathbf{r}_{ij} = \mathbf{r}_i - \mathbf{r}_j, \quad \mathbf{R}_k = \mathbf{r}_k - \frac{\mathbf{r}_i + \mathbf{r}_j}{2} \quad (9)$$

Therefore, the spatial symmetrical wave functions for exchanging any two identical quarks can be expressed as,

$$\Psi_{L_TM_T}(\mathbf{R},\mathbf{r}) = \sum_{i,j,k=1}^{3}{}' \left[\phi_{lm}(\mathbf{r}_{ij})\phi_{LM}(\mathbf{R}_k)\right]_{L_TM_T} \quad (10)$$

For other baryons, Λ, Σ, Σ^*, Ξ and Ξ^*, we assume that two identical quarks locate at positions $\mathbf{r}_1$ and $\mathbf{r}_2$, while the different quark locates at position $\mathbf{r}_3$, in this way, the spatial wave functions have the following form,

$$\Psi_{L_TM_T}(\mathbf{R},\mathbf{r}) = \left[\phi_{lm}(\mathbf{r}_{12})\phi_{LM}(\mathbf{R}_3)\right]_{L_TM_T} \quad (11)$$

The function $\phi_{lm}(\mathbf{r})$, $\phi_{LM}(\mathbf{R})$ are the superpositions of Gaussian basis functions with different sizes,

$$\begin{aligned} \phi_{lm}(\mathbf{r}) &= \sum_{n=1}^{n_{max}} c_n N_{nl} r^l e^{-\nu_n r^2} Y_{lm}(\hat{\mathbf{r}}) \quad (12) \\ \psi_{LM}(\mathbf{R}) &= \sum_{N=1}^{N_{max}} c_N N_{NL} R^L e^{-\nu_N R^2} Y_{LM}(\hat{\mathbf{R}}) \quad (13) \end{aligned}$$

where N_{nl} and N_{NL} are normalization constants. Gaussian size parameters are taken as geometric progression,

$$r_n = r_1 a^{n-1}, \quad \nu_n = \tfrac{1}{r_n^2}, \quad a = \left(\frac{r_{n_{max}}}{r_1}\right)^{\frac{1}{n_{max}-1}} \quad (14)$$

$$R_N = R_1 A^{N-1}, \quad \nu_N = \tfrac{1}{R_N^2}, \quad A = \left(\frac{R_{N_{max}}}{R_1}\right)^{\frac{1}{N_{max}-1}} \quad (15)$$

The numbers n and l (N and L) specify, respectively, the radial and angular momenta excitations with respect to the Jacobian coordinate $\mathbf{r}$ ($\mathbf{R}$). The angular momenta l and L are coupled to the total orbit angular momentum L_T. In the present work three angular momenta are assumed to be zero.

The model parameters are fixed as follows: the u,d-quark mass difference is neglected and m_u=m_d is assumed to be exactly $\frac{1}{3}$ of the nucleon mass, namely m_u=m_d=313 MeV. The parameters Λ_0 and μ_0 are taken from Ref. [30], namely $\Lambda_0 = 36.976$ MeV and $\mu_0 = 0.113$ fm, the rest parameters, α_0, K, β and m_s, are determined by fitting light baryon spectrum. Using above Hamiltonian and wave functions, the baryon spectrum can be obtained by solving the three-body Schrödinger equation

$$(H_3 - E)\Phi_{IM_IJM_J}(\mathbf{R},\mathbf{r}) = 0 \quad (16)$$

with Rayleigh-Ritz variational principle. The converged results, which are shown in Table I, are arrived by setting $r_1 = R_1 = 0.3$ fm, $r_{n_{max}} = R_{n_{max}} = 2.0$ fm and $n_{max} = N_{max} = 5$. The fitting parameters are $K = 336$ MeV·fm^{-2}, $\beta = 0.32$ fm, $m_s = 585$ MeV and $\alpha_0 = 6.82$.

TABLE I: Baryon spectrum (MeV).

State	N	Λ	Σ	Ξ	Δ	Σ^*	Ξ^*	Ω
Cal.	939	1022	1196	1307	1232	1397	1542	1673
Exp.	939	1116	1195	1315	1232	1384	1533	1672

III. SIX-BODY CONFINEMENT POTENTIAL AND WAVE FUNCTIONS

In the flux tube model it is assumed that the color-electric flux is confined to narrow, stringlike tubes joining quarks in accordance with Gauss's law. A flux tube starts from every quark and ends at an anti-quark or a Y-shaped junction, where the three flux tubes meet [32]. For $q^3\bar{q}^3$ system, it can be consisted of a color singlet baryon and a color singlet anti-baryon as in the usual hadron degree of freedom description, but also of a color octet baryon and a color octet anti-baryon coupled to an overall color singlet six quark state. The latter is called hidden color channel and because of color confinement, these hidden color channels exist in the two-cluster overlap region only. The $q^3\bar{q}^3$ systems have been studied in the usual constituent quark model, no bound state is found for non-strange system [33, 34]. Here the hidden color structure for $B\bar{B}$ system is considered. The flux-tube structure is shown in Fig. 1, in which $\mathbf{r}_i$ represents the position coordinate of the quark q_i (antiquark $\bar{q}_i$) which is denoted by a solid (hollow) dot, $\mathbf{y}_i$ represents a junction. A thin line connecting a quark and a junction represents a fundamental string, *i.e.* color triplet, a thick line connecting two junctions is for a color sextet, octet or others, namely a compound string.

Within the flux tube model, the confinement for a six-quark state can be written as

$$\begin{aligned} V^C &= K\left[(\mathbf{r}_1 - \mathbf{y}_1)^2 + (\mathbf{r}_2 - \mathbf{y}_1)^2 + (\mathbf{r}_3 - \mathbf{y}_2)^2 \right. \\ &+ (\mathbf{r}_4 - \mathbf{y}_3)^2 + (\mathbf{r}_5 - \mathbf{y}_4)^2 + (\mathbf{r}_6 - \mathbf{y}_4)^2 \quad (17) \\ &+ \left. \kappa_d\left((\mathbf{y}_1 - \mathbf{y}_2)^2 + (\mathbf{y}_2 - \mathbf{y}_3)^2 + (\mathbf{y}_3 - \mathbf{y}_4)^2\right)\right] \end{aligned}$$

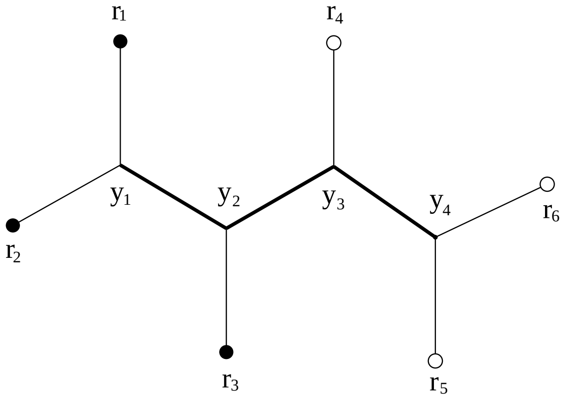

FIG. 1: Hidden color flux tube structure.

The string stiffness constant of an elementary or color triplet string is K, while $K\kappa_d$ is other compound string stiffness. The compound string stiffness parameter κ_d [35] depends on the color dimension, d, of the string,

$$\kappa_d = \frac{C_d}{C_3}, \tag{18}$$

where C_d is the eigenvalue of the Casimir operator associated with the $SU(3)$ color representation d on either end of the string, namely $C_3 = \frac{4}{3}$, $C_6 = \frac{10}{3}$ and $C_8 = 3$.

For given quark (antiquark) positions $\mathbf{r}_i$, those junction coordinates $\mathbf{y}_i$ are obtained by minimizing the confinement potential. By introducing the following set of canonical coordinates $\mathbf{R}_i$,

$$\begin{aligned}
\mathbf{R}_1 &= \frac{1}{\sqrt{2}}(\mathbf{r}_1 - \mathbf{r}_2), \qquad \mathbf{R}_2 = \frac{1}{\sqrt{2}}(\mathbf{r}_5 - \mathbf{r}_6) \\
\mathbf{R}_3 &= \frac{1}{\sqrt{12}}(\mathbf{r}_1 + \mathbf{r}_2 - 2\mathbf{r}_3 - 2\mathbf{r}_4 + \mathbf{r}_5 + \mathbf{r}_6) \\
\mathbf{R}_4 &= \frac{1}{\sqrt{33+5\sqrt{33}}}(\mathbf{r}_1 + \mathbf{r}_2 - \frac{5+\sqrt{33}}{2}\mathbf{r}_3 \\
&+ \frac{5+\sqrt{33}}{2}\mathbf{r}_4 - \mathbf{r}_5 - \mathbf{r}_6) \qquad (19) \\
\mathbf{R}_5 &= \frac{1}{\sqrt{33-5\sqrt{33}}}(\mathbf{r}_1 + \mathbf{r}_2 + \frac{\sqrt{33}-5}{2}\mathbf{r}_3 \\
&- \frac{\sqrt{33}-5}{2}\mathbf{r}_4 - \mathbf{r}_5 - \mathbf{r}_6) \\
\mathbf{R}_6 &= \frac{1}{\sqrt{6}}(\mathbf{r}_1 + \mathbf{r}_2 + \mathbf{r}_3 + \mathbf{r}_4 + \mathbf{r}_5 + \mathbf{r}_6),
\end{aligned}$$

the minimum of the confinement takes the following form,

$$\begin{aligned}
V^C_{min} &= K\left(\mathbf{R}_1^2 + \mathbf{R}_2^2 + \frac{3\kappa_d}{2+3\kappa_d}\mathbf{R}_3^2\right. \qquad (20) \\
&+ \left.\frac{2\kappa_d(\kappa_d+w_1)}{2\kappa_d^2+7\kappa_d+2}\mathbf{R}_4^2 + \frac{2\kappa_d(\kappa_d+w_2)}{2\kappa_d^2+7\kappa_d+2}\mathbf{R}_5^2\right)
\end{aligned}$$

where $w_1 = (7+\sqrt{33})/4, w_2 = (7-\sqrt{33})/4$,. The above expression gives only the interaction for pattern which is shown in Fig.1. The complete expression of confinement can be obtained by symmetrizing the above expression with respect to $\mathbf{r}_1, \cdots, \mathbf{r}_6$. Obviously, the confinement potential is multi-boy interaction rather than the sum of two-body one.

The model wave function can be expressed as,

$$\Psi^{B\bar{B}}_{I_T,J_T} = \sum c_\xi \left[\left[\Phi^B_{c_1IJ}\Phi^{\bar{B}}_{c_2I'J'}\right]_\xi F(\mathbf{X})\right]_{I_TJ_T} \tag{21}$$

$\Phi^B_{c_1IJ}$, $\Phi^{\bar{B}}_{c_2I'J'}$ are cluster wave functions of colorful baryon and anti-baryon, $[\cdots]_\xi$ represents all the needed coupling: color, isospin and spin. $F(\mathbf{X})$ is the relative orbital wave function between baryon and anti-baryon, in which $\mathbf{X}$ is the relative coordinate between baryon and anti-baryon center of mass coordinates $\mathbf{R}^B_C$ and $\mathbf{R}^{\bar{B}}_C$, namely $\mathbf{X} = \mathbf{R}^B_C - \mathbf{R}^{\bar{B}}_C$. all the possible channels are taken into account in our multichannel coupling calculation. Using GEM, the relative orbital wave function $F(\mathbf{X})$ can be expressed as,

$$F(\mathbf{X}) = \sum_{N'=1}^{N'_{max}} c_{N'}N_{N'L'}X^{L'}e^{-\nu_{N'}X^2}Y_{L'M'}(\hat{\mathbf{X}}) \tag{22}$$

In the calculation, all the orbital motions are assumed to be zero as before.

IV. NUMERICAL RESULTS AND DISCUSSIONS

Now we turn the attentions to the numerical calculation. The model parameters are fixed in fitting the ground state baryon spectrum, No new parameter is introduced in the six-body calculation. The eigen-energies and eigenfunctions of the $B\bar{B}$ system can be obtained by solving the six-body Schrödinger equation

$$(H_6 - E)\Psi^{B\bar{B}}_{I_TJ_T} = 0 \tag{23}$$

with Rayleigh-Ritz variational principle. The calculated results are converged with n_{max}=5, N_{max} = 5 and N'_{max} = 5. Minimum and maximum ranges of the bases are 0.3 fm and 2.0 fm for coordinates $\mathbf{r}$, $\mathbf{R}$ and $\mathbf{X}$, respectively.

Multichannel coupling results for non-strange six-quark states with all possible quantum numbers are listed in Table II, where only the lowest mass is shown for each set of quantum numbers. In the table, the superscript (subscript) of $N(\Delta)$ represents spin quantum number and color dimensions. The Pauli forbidden states are not listed in the table.

In the present calculation, the one-boson-exchange interactions are not invoked, the channel coupling effective in Table II is induced by one gluon exchange interaction. For the sake of discussion, the results reclassified in terms of baryon category is shown in Table III.

TABLE II: Numerical results for $B\bar{B}$ systems (MeV).

I^GJ^{PC}	Mass	Coupled channels
0^+0^{-+}	1851	$N_8^{\frac{1}{2}}\bar{N}_8^{\frac{1}{2}}$, $\Delta_8^{\frac{1}{2}}\bar{\Delta}_8^{\frac{1}{2}}$, $N_8^{\frac{3}{2}}\bar{N}_8^{\frac{3}{2}}$
0^-1^{--}	2068	$N_8^{\frac{1}{2}}\bar{N}_8^{\frac{1}{2}}$, $N_8^{\frac{1}{2}}\bar{N}_8^{\frac{3}{2}}$, $\Delta_8^{\frac{1}{2}}\bar{\Delta}_8^{\frac{1}{2}}$, $N_8^{\frac{3}{2}}\bar{N}_8^{\frac{1}{2}}$, $N_8^{\frac{3}{2}}\bar{N}_8^{\frac{3}{2}}$,
0^+2^{-+}	2226	$N_8^{\frac{1}{2}}\bar{N}_8^{\frac{3}{2}}$, $N_8^{\frac{3}{2}}\bar{N}_8^{\frac{1}{2}}$, $N_8^{\frac{3}{2}}\bar{N}_8^{\frac{3}{2}}$
0^-3^{--}	2638	$N_8^{\frac{3}{2}}\bar{N}_8^{\frac{3}{2}}$
1^-0^{-+}	1851	$N_8^{\frac{1}{2}}\bar{N}_8^{\frac{1}{2}}$, $N_8^{\frac{1}{2}}\bar{\Delta}_8^{\frac{1}{2}}$, $\Delta_8^{\frac{1}{2}}\bar{N}_8^{\frac{1}{2}}$, $\Delta_8^{\frac{1}{2}}\bar{\Delta}_8^{\frac{1}{2}}$, $N_8^{\frac{3}{2}}\bar{N}_8^{\frac{3}{2}}$
1^+1^{--}	2068	$N_8^{\frac{1}{2}}\bar{N}_8^{\frac{1}{2}}$, $N_8^{\frac{1}{2}}\bar{\Delta}_8^{\frac{1}{2}}$, $N_8^{\frac{1}{2}}\bar{N}_8^{\frac{3}{2}}$, $\Delta_8^{\frac{1}{2}}\bar{N}_8^{\frac{1}{2}}$, $\Delta_8^{\frac{1}{2}}\bar{\Delta}_8^{\frac{1}{2}}$
		$\Delta_8^{\frac{1}{2}}\bar{N}_8^{\frac{3}{2}}$, $N_8^{\frac{3}{2}}\bar{N}_8^{\frac{1}{2}}$, $N_8^{\frac{3}{2}}\bar{\Delta}_8^{\frac{1}{2}}$, $N_8^{\frac{3}{2}}\bar{N}_8^{\frac{3}{2}}$,
1^-2^{-+}	2226	$N_8^{\frac{1}{2}}\bar{N}_8^{\frac{3}{2}}$, $\Delta_8^{\frac{1}{2}}\bar{N}_8^{\frac{3}{2}}$, $N_8^{\frac{3}{2}}\bar{N}_8^{\frac{1}{2}}$, $N_8^{\frac{3}{2}}\bar{\Delta}_8^{\frac{1}{2}}$, $N_8^{\frac{3}{2}}\bar{N}_8^{\frac{3}{2}}$
1^+3^{--}	2638	$N_8^{\frac{3}{2}}\bar{N}_8^{\frac{3}{2}}$
2^+0^{-+}	2415	$N_8^{\frac{1}{2}}\bar{\Delta}_8^{\frac{1}{2}}$, $\Delta_8^{\frac{1}{2}}\bar{N}_8^{\frac{1}{2}}$, $\Delta_8^{\frac{1}{2}}\bar{\Delta}_8^{\frac{1}{2}}$
2^-1^{--}	2380	$N_8^{\frac{1}{2}}\bar{\Delta}_8^{\frac{1}{2}}$, $\Delta_8^{\frac{1}{2}}\bar{N}_8^{\frac{1}{2}}$, $\Delta_8^{\frac{1}{2}}\bar{\Delta}_8^{\frac{1}{2}}$, $\Delta_8^{\frac{1}{2}}\bar{N}_8^{\frac{3}{2}}$, $N_8^{\frac{3}{2}}\bar{\Delta}_8^{\frac{1}{2}}$
2^+2^{-+}	2596	$N_8^{\frac{3}{2}}\bar{\Delta}_8^{\frac{1}{2}}$, $\Delta_8^{\frac{1}{2}}\bar{N}_8^{\frac{3}{2}}$
3^-0^{-+}	2415	$\Delta_8^{\frac{1}{2}}\bar{\Delta}_8^{\frac{1}{2}}$
3^+1^{--}	2760	$\Delta_8^{\frac{1}{2}}\bar{\Delta}_8^{\frac{1}{2}}$

TABLE III: Masses for $N_8\bar{N}_8$, $N_8\bar{\Delta}_8$ and $\Delta_8\bar{\Delta}_8$ (MeV).

IJ	00	01	02	03	10	11	12	13
$N_8\bar{N}_8$	1851	2068	2226	2638	1851	2068	2226	2638
IJ	10	11	12	13	20	21	22	23
$N_8\bar{\Delta}_8$	2546	2380	2596	—	2546	2380	2596	—
IJ	00	10	20	30	01	11	21	31
$\Delta_8\bar{\Delta}_8$	2415	2415	2415	2415	2760	2760	2760	2760

For $N_8\bar{N}_8$ and $\Delta_8\bar{\Delta}_8$ states in Table III, it can be seen that the masses of the states with the only different isospin I are degeneracy due to the absence of one-boson-exchange interaction. The states $N_8\bar{N}_8$ and $\Delta_8\bar{\Delta}_8$ with the same $I^GJ^{PC} = 0^+0^{-+}$ have the lowest energies 1851 MeV and 2415 MeV, respectively. They are bound states because their energies are lower than the corresponding thresholds of $N\bar{N}$ and $\Delta\bar{\Delta}$. One gluon exchange provide a strong attractive force for $\Delta_8\bar{\Delta}_8$, which is of benefit to form a bound state. The mass of $\Delta_8\bar{\Delta}_8$ state close to the energy of newly observed state $X(2370)$, so it is possible to interpret $X(2370)$ as $\Delta_8\bar{\Delta}_8$ state with $I^GJ^{PC} = 0^+0^{-+}$.

$N_8\bar{N}_8$ is consisted of two channels $N_8^{\frac{1}{2}}\bar{N}_8^{\frac{1}{2}}$ and $N_8^{\frac{3}{2}}\bar{N}_8^{\frac{3}{2}}$, the single-channel calculations give the energy of the former 2324 MeV and the latter 2180 MeV. However, the channel coupling is strong and the energy of the lower eigen-state is reduced to 1851 MeV, which is very close to the mass of newly observed state $X(1835)$. Assigning $X(1835)$ to the hidden color state $N\bar{N}$ with quantum numbers $I^GJ^{PC} = 0^+0^{-+}$ is favored in the present calculation.

For $N_8\bar{\Delta}_8$ states, the lowest energy channel is not $I^GJ^{PC} = 1^-0^{-+}$ but $I^GJ^{PC} = 1^+1^{--}$ because more channels are involved in the latter case (see Table II). $N\bar{\Delta}$ can not form a bound state because the lowest eigen-energy 2380 MeV is still higher than the corresponding threshold of $N\bar{\Delta}$.

Comparing with two-body confinement one proportional to color factor $\lambda_i^c \cdot \lambda_j^c$, in general, the multi-body one depress the energy of a system more 100 MeV [20], which is advantageous to the formation of a bound state.

TABLE IV: Rms for $N_8\bar{N}_8$ and $\Delta_8\bar{\Delta}_8$ (fm).

Distances	$\langle(\mathbf{r}_i - \mathbf{R}_C^B)^2\rangle^{\frac{1}{2}}$	$\langle(\mathbf{r}_j - \mathbf{R}_C^{\bar{B}})^2\rangle^{\frac{1}{2}}$	$\langle\mathbf{X}^2\rangle^{\frac{1}{2}}$
$N_8\bar{N}_8$	0.60	0.60	0.49
$\Delta_8\bar{\Delta}_8$	0.64	0.64	0.59

Using the wave functions of states $N_8\bar{N}_8$ and $\Delta_8\bar{\Delta}_8$, the roots mean square (rms) of the systems are calculated and given in Table IV, where $i \in B_8$ and $j \in \bar{B}_8$. It can be seen from Table IV that the radius of B_8 ($\bar{B}_8$) is about 0.6 fm, Δ_8 ($\bar{\Delta}_8$) is a little greater than N_8 ($\bar{N}_8$), the distances between N_8 and $\bar{N}_8$, Δ_8 and $\bar{\Delta}_8$ are 0.49 fm and 0.59 fm, respectively. The two colorful clusters are highly overlapped. Therefore, with above assignment, $X(1835)$ and $X(2370)$ are compact six-quark states with three-dimensional configurations similar to American football.

The hidden color stats $X(1835)$ and $X(2370)$ can decay into $\eta'\pi^+\pi^-$, the process of transforming into several color singlet mesons proceeds by means of breaking and rejoining flux tubes. This decay mechanism is similar to compound nucleus formation and therefore should induce a resonance which is named as a "color confined, multi-quark resonance" state [36] in our model, it is different from all of those microscopic resonances discussed by S. Weinberg [37]. Bicudo and Cardoso also found plausible the existence of resonances in which the tetraquark component originated by a flip-flop potential is the dominant one [38].

V. SUMMARY

By using high precision few-body calculation method GEM, non-strange baryonium formed by two colorful clusters, B_8 and $\bar{B}$, is studied in the flux tube model with a six-body confinement potential. The energies of the states $N_8\bar{N}_8$ and $\Delta_8\bar{\Delta}_8$ with $I^GJ^{PC} = 0^+0^{-+}$ are 1851 MeV and 2415 MeV, which are lower than the thresholds of $N\bar{N}$ and $\Delta\bar{\Delta}$, respectively. they could be "color confined, multi-quark resonance" states. The newly observed $X(1835)$ and $X(2370)$ can explained as $N_8\bar{N}_8$ and $\Delta_8\bar{\Delta}_8$ bound states, $X(2120)$ can be accommodated in our model. The radius of B_8 ($\bar{B}_8$) is about 0.6 fm, Δ_8 ($\bar{\Delta}_8$) is a little greater than N_8 ($\bar{N}_8$), the distances between N_8 and ($\bar{N}_8$), Δ_8 and ($\bar{\Delta}_8$) are 0.49 fm and 0.59 fm, respectively. Therefore, $X(1835)$ and $X(2370)$ are compact six-quark states with three-dimensional configurations similar to American football.

There are many problems remained and need to be studied further, channel coupling calculation containing all possible flux tube structures should be done, the crucial test of the structures of exotic hadrons is determined by the systematic study of their decays, both are based on a Hamiltonian including the transition interaction which is responsible for changing flux tube structures by means of the creation, annihilation and arrangement of flux tubes.

Acknowledgments

This work is supported partly by the National Science Foundation of China under Contract Nos. 11047140, 11175088, 11035006, 11047023, and the Ph.D Program Funds of Chongqing Jiaotong University.

[1] J. Z. Bai et al. (BES Collaboration), Phys. Rev. Lett. **91**, 022001 (2003).
[2] M. Ablikim et al. (BES Collaboration), Phys. Rev. Lett. **95**, 262001 (2005).
[3] M. Ablikim et al. (BES Collaboration), Phys. Rev. Lett. **106**, 072002 (2011).
[4] A. Datta and P. J. O'Donnell, Phys. Lett. B **567**, 273 (2006).
[5] G. J. Ding and M. L. Yan, Phys. Rev. C **72**, 015208 (2005).
[6] C. S. Gao and S. L. Gao, Commun. Theor Phys. **42**, 844 (2004).
[7] N. Kochelev and D. P. Min, Phys. Lett. B **633**, 283 (2006).
[8] X. G. He, X. Q. Li, X. Liu and J. P. Ma, Eur. Phys. J. C **49**, 731 (2007)
[9] B. A. Li, Phys. Rev. D **74**, 034019 (2006).
[10] G. J. Ding and M. L. Yan, Eur. Phys. J. A **28**, 351 (2006).
[11] C. Liu, Eur. Phys. J. C **53**, 413 (2008).
[12] T. Huang and S. L. Zhu, Phys. Rev. D **73**, 014023 (2006).
[13] D. R. Entem and F. Fernández, Phys. Rev. C **73**, 045214 (2006).
[14] J. S. Yu, Z. F Sun, X. Liu and Q. Zhao, Phys. Rev. D **83**, 114007 (2011).
[15] P. Maris and C. R. Roberts, Int. J. Mod. Phys. E **12**, 297 (2003).
[16] N. Ishii, S. Aoki, and T. Hatsuda, Phys. Rev. Lett. **99**, 022001 (2007).
[17] T. T. Takahashi and Y. Kanada-En'yo, Phys. Rev. D **82**, 094506 (2010).
[18] S. Godfrey, J. Napolitano, Rev. Mod. Phys. **71**, 5 (1999).
[19] J. L. Ping, C. R. Deng, F. Wang and T. Goldman, Phys. Lett. B **659**, 607 (2008).
[20] C. R. Deng, J. L. Ping, F. Wang and T. Goldman, Phys. Rev. D **82**, 074001 (2010).
[21] F. Wang and C. W. Wong, Nuovo Cimento A **86**, 283 (1985).
[22] O. W. Greenberg and H. J. Lipkin, Nucl. Phys. A **370**, 349 (1981).
[23] M. Oka, Phys. Rev. D **31**, 2274 (1985).
[24] M. Oka and C. J. Horowitz, Phys. Rev. D **31**, 2773 (1985).
[25] V. Dmitrasinovic, Phys. Rev. D **67**, 114007 (2003).
[26] C. Alexandrou, P. De Forcrand and A. Tsapalis, Phys. Rev. D **65**, 054503 (2002);
T. T. Takahashi, H. Suganuma, Y. Nemoto, and H. Matsufuru, Phys. Rev. D **65**, 114509 (2002);
F. Okiharu, H. Suganuma and T. T. Takahashi, Phys. Rev. D **72**, 014505 (2005);
[27] F. Okiharu, H. Suganuma and T. T. Takahashi, Phys. Rev. Lett. **94**, 192001 (2005).
[28] T. Goldman and S. Yankielowicz, Phys. Rev. D 12, 2910 (1975).
[29] C. R. Deng, J. L. Ping and F. Wang, Eur. J. Phys. C (submitted).
[30] J. Vijande, F. Fernandez and A. Valcarce, J. Phys. G **31**, 481 (2005).
[31] J. Weinstein, N. Isgur, Phys. Rev. D **27**, 588 (1983).
[32] N. Isgur and J. Paton, Phys. Rev. D **31**, 2910 (1985).
[33] D. R. Entem and F. Fernandez, Phys. Rev. C **73**, 045214 (2006).
[34] H. X. huang, H. R. Pang and J. L. Ping, Mod. Phys. Lett. A **26**, 1231 (2011).
[35] G. S. Bali, Phys. Rev. D **62**, 114503 (2000).
[36] Fan Wang, J.L. Ping, H.R. Pang and L.Z. Chen, Nuclear Physics A **790**, 493cC497c(2007).
[37] S. Weinberg, *The Quantum Theory of Fields*, (Combridge University Press, 1995), V.I, p.159.
[38] P. Bicudo and M. Cardoso, Phys. Rev. D **83**, 094010 (2011).